Efficiently simulating personal vehicle energy consumption in mesoscopic transport models

Zachary A. Needell
Institute for Data, Systems, and Society
Department of Civil and Environmental Engineering
Massachusetts Institute of Technology
77 Massachusetts Avenue Cambridge, MA 02139
Email: zneedell@mit.edu

Jessika E. Trancik (Corresponding Author)
Institute for Data, Systems, and Society
Massachusetts Institute of Technology
77 Massachusetts Avenue Cambridge, MA 02139
Santa Fe Institute
Santa Fe, New Mexico 87501
Phone: 617-715-4552, Fax: 617-258-7733, Email: trancik@mit.edu

Word Count: 6,500 words + 2 figures + 2 tables = 7,500 words
Submission Date: February 7, 2018

Abstract
Mesoscopic transport models can efficiently simulate complex travel behavior and traffic patterns over large networks, but simulating energy consumption in these models is difficult with traditional methods. Since mesoscopic transport models rely on a simplified handling of traffic flow, they cannot provide the second-by-second measurement of vehicle speeds and accelerations that are required for accurately estimating energy consumption. Here we present extensions to the TripEnergy model that fill in the gaps of low-resolution trajectories with realistic, contextual driving behavior. TripEnergy also includes a vehicle energy model capable of simulating the impact of traffic conditions on energy consumption and CO_2 emissions, with inputs in the form of widely-available calibration data, allowing it to simulate thousands of different real-world vehicle makes and models. This design allows TripEnergy to integrate with mesoscopic transport models and to be fast enough to run on a large network with minimal additional computation time. We expect it to benefit from and enable advances in transport simulation, including optimizing traffic network controls to minimize energy, evaluating the performance of different vehicle technologies under wide-scale adoption, and better understanding the energy and climate impacts of new infrastructure and policies.

INTRODUCTION

A variety of transport simulation models allow researchers and policymakers to predict the behavior of travelers in great detail under different policy, infrastructure, and travel demand scenarios. Producing energy-use and emissions estimates with these models opens up an even larger set of possible research and policymaking applications—from estimating the emissions implications of different policies or traffic control strategies to evaluating the expected usage patterns of emerging vehicle technologies. However, barriers still remain to widespread application of linked transport and energy/emissions models. In this paper, we present a new, flexible energy model calibrated on a large sample of GPS driving behavior data and capable of linking with a mesoscopic transport model to efficiently produce energy estimates for personal vehicles on large transport networks.

To be widely applicable to transport simulation, an energy model must balance efficiency and specificity (*1*). Increases in computational power allow city-sized transport networks to be simulated at the agent level—capturing the travel-related decisions and movements of millions of travelers at a seconds time-scale. These models can simulate congestion, trip-making decisions, and traveler response to information and incentives to a degree that is fundamentally impossible with simpler models. The massive scale of these simulations requires that any energy model at the vehicle scale operate very quickly and with minimal memory overhead. However, the large number of different vehicle types on the road and the variety of operating conditions they face during real-world use also require that any energy model either depends on vast amounts of calibration data or incorporates simplifications. While striking this balance, a useful model must capture the relationship of vehicle energy use to the congestion, driver behavior, and external conditions that motivate the use of detailed transport models in the first place.

Here we present an extension of the existing TripEnergy model (*2*), allowing for the efficient linking of a mesoscopic transport simulation model with an energy model calibrated to reproduce real-world energy use for a wide range of personal vehicles. By relying primarily on empirical observations and simple physical approximations, this energy model uses fewer tunable parameters than other methods. It neither requires high-resolution simulation of individual vehicle motion, nor does it use traffic flow theory to fill in the gaps of the moderate-resolution vehicle trajectories produced by more computationally efficient mesoscopic models. Both of these alternative approaches require calibration against disaggregate data that, while available for traffic counts and speeds, are far more difficult to incorporate when the error to be minimized is against energy consumption (*3*). Instead, the model presented here draws from a database of over 100,000 GPS speed histories taken from various statewide travel surveys of real-world drivers (*2, 4-6*) and fills in the gaps of moderate-resolution simulated trajectories with representative examples of realistic high-resolution driving behavior. This energy model also does not require detailed emission rates as inputs, instead using a simple vehicle energy model that can be calibrated on widely-available regulatory data but that still reproduces energy consumption accurately enough for most purposes, allowing thousands of individual vehicle types to be simulated with minimal additional calibration. It achieves sufficient computational efficiency to run on large-scale networks through a novel separation of the driving behavior and vehicle performance steps of the energy estimation procedure.

This paper outlines the extensions to TripEnergy that allow it to efficiently process mesoscopic transportation model outputs, describes a validation procedure for the matching method and energy estimates, and presents results of simulation on a test network. We describe the energy estimation procedure in two steps—a vehicle model that translates characteristics of a

high-resolution trajectory into an energy estimate, and a driving behavior model that links moderate-resolution simulated vehicle trajectories to a database of high-resolution trajectories. Model validation is performed by downsampling drive cycles to moderate resolution and then application of the driving behavior and vehicle models, comparing results to energy estimates given full knowledge of the trajectory and a much more detailed vehicle simulation (*7*) and dynamometer results (*8*). The model is then linked to the SimMobility mesoscopic transport simulation model (*9*) and results are examined for a toy road network, reproducing expected energy performance for a range of different real-world vehicle models.

BACKGROUND

Traffic Network Modeling

Transport models work by considering the relationship between transportation supply and demand. The characteristics of the road and transit network such as travel times and costs are considered in the supply model, while the demand model considers the destinations, departure times, modes, and route choices for individuals' trips. For supply, dynamic traffic assignment (DTA) moves vehicles through the traffic network based on real-time traffic conditions (*10*). Implementations of this method are able to capture certain effects, such as gridlock, queuing, and rerouting, which cannot be easily modeled using static methods. Some vehicle-following models directly simulate acceleration, lane changing, and gap-acceptance, and, given extensive calibration, can reproduce the realistic high-resolution vehicle trajectories necessary to estimate energy use. However, even if such calibration data exist, which is often not the case, it remains infeasible to run such detailed models on large networks. As an alternative, "mesoscopic models" are able to capture many of the complex aspects of transport supply while still achieving sufficient computational efficiency to run on large networks. Mesoscopic models also follow individual agents across the network, but they contain a simplified treatment of vehicle movement and often operate at a lower temporal resolution, typically on the order of five to fifteen seconds. While sacrificing some details such as variability in driving style and complex interactions between vehicles, such mesoscopic methods have been successfully applied to large networks (*11*) and can run quickly enough to optimize controls (*12*). Mesoscopic traffic supply is included in many transport simulation models, such as SimMobility Midterm (*9*), DTAlite (*13*), and MATSIM (*14*).

For demand, most state-of-the-art models are "activity based." Unlike more traditional methods, activity based models simulate individual travelers' trip-making decisions in terms of how they allow travelers to complete a daily sequence of activities. Because they track traveler location and choices throughout the day, activity based models can capture more realistic feedback between transportation network performance and travel demand (*15*). Energy modeling is more closely related to the supply side of the modeling framework, but certain questions can be fully answered only by integrating energy calculations directly into the supply/demand interaction. For example, the limited range of existing battery-electric vehicles means that charging requirements will likely become a greater component of travel decision-making, motivating development of energy models that can run in concert with transport supply and demand calculations.

Vehicle Modeling

Transport models implicitly or explicitly simulate vehicle movement, and there exist various software tools to turn simulated trajectories into energy estimates given a vehicle type. These

characterizations of vehicle movement can vary in terms of their temporal resolution and the fidelity with which they can be expected to represent real driving behavior, leading to different scales at which energy models must operate. The characteristics of selected models are summarized in Table 1.

Most traditional transport simulations model supply based on average speeds and densities of road network links. These link-level speeds can be turned into energy estimates by models such as COPERT (*16*) that rely on empirical measurements of typical energy and emissions rates but do not directly capture the local effects of accelerations on energy use. Link speeds can also be aggregated into beginning-to-end trip average speeds, which can be used to estimate energy consumption by models such as EMFAC (*17*).

If a network simulation produces high-resolution trajectories (typically 1 Hertz or greater), those trajectories can be fed into detailed vehicle simulations such as ADVISOR (*7*). These models simulate the mechanics of vehicles in great detail and are best equipped to simulate complicated processes such as criterion pollutant emissions or engine performance under extreme operating conditions. However, these detailed models are slow to run, making them impractical to run on the output of large network simulations.

To achieve greater efficiency while still capturing the detail provided by high-resolution trajectories, researchers have developed simpler models to approximate vehicle performance. Some estimate energy consumption rates based on polynomial fits to instantaneous speed (*16*) and others use fits based on speed and acceleration, including the widely-used VT-Micro model (*18*). To better incorporate factors such as road grade, a number of models estimate energy and emissions rates using vehicle specific power (VSP), a measure of the relative of the engine. One commonly used VSP-based model is CMEM (*19*), which relies on measurements from a variety of different vehicle types that cover the breadth of models in the on-road vehicle fleet. Other vehicle models, some requiring less calibration data, have been proposed and evaluated as well (*20*).

One particularly comprehensive and widely-used energy and emissions model is MOVES (*21*), which uses a database of emissions rates for a large number of different vehicle types over a variety of speed and VSP bins known as operating modes. The distribution of time spent in each of these operating mode bins is estimated based on a combination of disaggregate speed, temperature, travel behavior, and vehicle fleet data. MOVES can be cumbersome to run at its most detailed settings, so for the added efficiency and flexibility others have developed a simplified version, MOVESLite (*22*), with a more limited but still comprehensive set of vehicle types and operating modes.

In all of these cases, there is an underlying difficulty: Efficient simulation of large networks requires some sort of simplification in the treatment of traffic flow, but energy consumption modeling requires a high-resolution representation of vehicle movement. This tradeoff is apparent in the various available levels of detail in MOVES. At the “County” level, MOVES populates its operating mode distribution table with results from a small set of high-resolution drive cycles. It then calculates emissions by weighting and aggregating emissions rates of these operating modes based on traffic patterns. This method, however, is not capable of directly simulating individual vehicle consumption or taking advantage of the full level of detail present in simulated mesoscopic trajectories. At the higher-detail “Project” level, however, MOVES requires drive schedules or operating mode distributions for each road link. To provide these inputs, it is necessary either to run a full high-resolution simulation of the network or to rely on default values that do not reflect local traffic conditions. This means that there is no widely-

used energy estimation methodology that is capable of taking advantage of both the computational efficiency of mesoscopic models as well as their ability to capture individual vehicle trajectories at a higher resolution than link average speeds. More recently, some researchers have proposed inferring detailed trajectory information from the moderate-resolution trajectories produced by mesoscopic network simulations. This approach has been implemented (*23, 24*) using traffic flow theory to model the acceleration behavior of drivers and then inferring vehicle specific power from these interpolated trajectories. The method we present has three main differences. First, TripEnergy fills in the details of mesoscopic trajectories with empirical, real-world behavior, requiring fewer calibration parameters. Second, it is designed to simulate the energy consumption of a large number of real-world vehicle types without needing large amounts of calibration data for each one. And, third, it uses a simpler model of instantaneous vehicle energy use, trading the ability to simulate emission of non-CO_2 pollutants and engine performance under extreme operating conditions to allow for more flexible and efficient implementation using a linear model.

METHODS

Vehicle Model

Drive Energy

This method of calculating energy consumption from a high-resolution trajectory relies on a simplification that allows the important aspects of the trajectory to be stored in a vehicle-independent manner but allows energy consumption for any vehicle type to be efficiently calculated from those stored values. The basis for the energy model is the version presented in a previous paper (*2*) and applied to questions of range constraints in battery electric vehicles (*25*), but reformulated here to depend only on instantaneous quantities. Unlike other pollutants such as CO and particulate matter, CO_2 emissions from a gasoline-powered vehicle are almost precisely linearly related to the energy content of the fuel, allowing this method to also estimate CO_2 emissions from gasoline-powered vehicles.

The basis for the energy calculations is the tractive power, a function of the vehicle's instantaneous speed v, acceleration a, and road grade θ, as well as its mass m, a set of polynomial coastdown coefficients A, B, and C, and a rotational inertia fraction ε, set to be 0.05 here (*26*):

$$\mathscr{P}_{tr}(t) = Av(t) + Bv(t)^2 + Cv(t)^3 + (1+\varepsilon)mv(t)a(t) + mg\sin(\theta(t))v(t) \quad (1)$$

In this paper, final energy quantities are written in script, whereas pre- conversion energy values (measured at the battery or gas tank) are written in normal font.

The rate of change of stored energy in the gas tank or in the battery consists of power going to the wheels, returning via the brakes (if regenerative braking exists), and going towards auxiliary electronics such as climate control. All of these processes involve conversion losses, taken into account with loss functions $P = L(\mathscr{P})$. The rate of change of stored energy is the power going towards motion $P_{accel} = L_{accel}(\mathscr{P}_{tr})$ minus the power sourced from regenerative brakes $P_{brake} = L_{brake}(\mathscr{P}_{tr})$, plus power going to the auxiliaries $P_{aux} = L_{aux}(\mathscr{P}_{aux})$, which depends on climate control and dashboard settings.

For clarity, we can define an indicator function for whether tractive power is positive (and the engine is active) or negative (and the brakes are active):

$$PTF(t) = \begin{cases} 1 & \mathscr{P}_{tr}(t) > 0 \\ 0 & \mathscr{P}_{tr}(t) \leq 0, \end{cases} \tag{2}$$

Finally, we make the further simplifying assumption that all loss functions are linear and that auxiliary power is constant over the course of a trip. The linear approximation has been shown to be reasonably accurate for internal combustion engine vehicles (*27*), and the framework we present here can easily be adjusted to allow for higher order polynomial terms, such as those tested by Saerens et al. (*20*). Using the linear approximation we have $L_{accel}(\mathscr{P}_{tr}(t)) = P_{idle} + \frac{\mathscr{P}_{tr}(t)PTF(t)}{\eta_{max}}$, $L_{brake}(\mathscr{P}_{tr}(t)) = \eta_{brake}\mathscr{P}_{tr}(t)(1 - PTF(t))$, and $L_{aux} = \frac{\mathscr{P}_{aux}}{\eta_{aux}}$. P_{idle} is the rate of energy use at no tractive power (including rest and coasting), effectively accounting for lower engine efficiency at low power. η_{max} is the slope of the $\mathscr{P}_{tr}$-P_{tr} line, effectively giving the engine efficiency approached at higher power. η_{brake} is the portion of energy going through the brakes re-cycled into the vehicle's battery and then back to the wheels. Defining the acceleration energy and braking energy as

$$\mathscr{E}_{accel} = \int_{t=0}^{T} \mathscr{P}_{tr}(t)PTF(t)dt; \quad \mathscr{E}_{brake} = \int_{t=0}^{T} -\mathscr{P}_{tr}(t)\,(1 - PTF(t))\,dt, \tag{3}$$

we can simplify the total energy equation:

$$E_{use} = \frac{\mathscr{E}_{accel}}{\eta_{max}} - \eta_{brake}\mathscr{E}_{brake} + \left(P_{idle} + \frac{\mathscr{P}_{aux}}{\eta_{aux}}\right)T. \tag{4}$$

This function for $\mathscr{E}_{accel}$ is dependent on the distance traveled and the average speed of the trip, so we can separate out the effects of these quantities by replacing t, $v(t)$ and $a(t)$ with unitless quantities: $\tau = (t - t_0)/T$, $u(\tau) = v(\tau)/\bar{v}$, and $\alpha(\tau) = a(\tau)/a_0$, where T is the total duration of the drive cycle, $\bar{v}$ is its average speed, and a_0 is a characteristic acceleration, defined as 0.15 m/s^2.

We can express the equation for $\mathscr{E}_{accel}$ by defining a set of 'moments' consisting of the time-integrals of these unitless quantities:

$$\mu_1 = \int_{\tau=0}^{1} u(\tau)PTF(\tau)d\tau \qquad \mu_2 = \int_{\tau=0}^{1} u(\tau)^2PTF(\tau)d\tau$$
$$\mu_3 = \int_{\tau=0}^{1} u(\tau)^3PTF(\tau)d\tau \qquad \mu_a = \int_{\tau=0}^{1} \alpha(\tau)u(\tau)PTF(\tau)d\tau \tag{5}$$

These definitions allow us to express the total acceleration energy without any integrals:

$$\mathscr{E}_{accel} = D\left(A\mu_1 + B\bar{v}\mu_2 + C\bar{v}^2\mu_3 + (1+\varepsilon)m\alpha_0\mu_a + mg\Delta Z\mu_1\right) \tag{6}$$

where D is total distance. For the road grade component, and we assume that road grade is relatively constant over each time interval, leaving the energy impact dependent on the total elevation change ΔZ. Braking energy is calculated similarly for $PTF(t) < 0$, for which we define the comparable moments as ν_i:

$$\mathscr{E}_{brake} = -D\left(A\nu_1 + B\bar{v}\nu_2 + C\bar{v}^2\nu_3 + (1+\varepsilon)m\alpha_0\nu_a + mg\Delta Z\nu_1\right). \quad (7)$$

These two equations and an estimate of auxiliary power yield total energy consumption via Equation 4. Pulling these average quantities outside of the integral effectively treats total energy consumption as a linear combination of these average quantities multiplied by correction factors that depend on the specific details of the true speed history. The final expression for energy consumption is a linear combination of ten terms relating to the vehicle and its use:

$$\mathbf{V} = \begin{bmatrix} A/\eta_{max} \\ B/\eta_{max} \\ C/\eta_{max} \\ (1+\varepsilon)m/\eta_{max} \\ A\eta_{brake} \\ B\eta_{brake} \\ C\eta_{brake} \\ (1+\varepsilon)m\eta_{brake} \\ P_{idle} \\ 1/\eta_{aux} \end{bmatrix}; \quad \mathbf{U} = D \begin{bmatrix} 1 \\ \bar{v} \\ \bar{v}^2 \\ 1 \\ -1 \\ -\bar{v} \\ -\bar{v}^2 \\ -1 \\ 1/\bar{v} \\ \mathscr{P}_{aux}/\bar{v} \end{bmatrix} \circ \begin{bmatrix} \mu_1 \\ \mu_2 \\ \mu_3 \\ \alpha_0\mu_a \\ \nu_1 \\ \nu_2 \\ \nu_3 \\ \alpha_0\nu_a \\ 1 \\ 1 \end{bmatrix}; \quad E_{drive} = \sum_{k=1}^{10} V_k U_k. \quad (8)$$

These moments are a helpful way of expressing the total energy because they are almost independent of vehicle type. This is a simplification only because the function $PTF(t)$ varies slightly from vehicle to vehicle, but these differences end up having little effect on the total energy and are ignored here. The moments, calculated for a partial or full vehicle trajectory, can serve a similar purpose to the link-specific driving schedules or operating mode distributions required as an input to MOVES, defining the factors of a vehicle's use that determine energy requirements. Rather than querying a detailed set of vehicle-specific emissions rates or evaluating integrals, all that is needed to evaluate this energy function is to access these stored parameters that can be calculated in advance, allowing for faster computation.

Drive Efficiency Calibration

The vehicle-specific component of the total energy in Equation 8, $\mathbf{V}$, depends in part on physical vehicle road load characteristics A, B, C, m that are publically available (*28*). The remaining three parameters, P_{idle}, η_{max}, and η_{brake} are estimated by fitting to energy consumption over a set of EPA test cycle results, similar to methods used elsewhere (*2, 20, 25*). We minimize mean squared error between the predicted (*MPGest*) and measured (*MPG*) fuel economy values for a set of test cycles *DC* with known fuel economy:

$$\underset{P_{idle},\eta_{max},\eta_{brake}}{\operatorname{argmin}} \sum_{i \in DC} \left(MPG_i - MPGest_i(P_{idle}, \eta_{max}, \eta_{brake})\right)^2. \quad (9)$$

For light duty vehicles, these drive cycles can consist of the EPA city (FTP) and highway (HWFET) drive cycles, as well as for the high speed (US06) cycle for the vehicles with it available. For this paper, we calibrate these parameters for 3,784 vehicle types with model years from 2010 to 2016. During calibration, P_{brake} is fixed to 0 for vehicles without regenerative braking. For vehicles with regenerative braking but only two test cycles available, P_{idle} is fixed—to 1409 W for hybrid electric vehicles and 741 W for fully electric vehicles—to ensure a unique solution. The value for hybrid electric vehicles is chosen by taking the median fit value for P_{idle} of the hybrid vehicles for which three unique fuel economy estimates are available. The value for fully electric vehicles is fixed to the value for P_{idle} found by calibrating the 2013 Nissan Leaf on

additional drive cycles whose energy consumption is provided in the Downloadable Dynamometer Database (*8*).

Each vehicle being simulated in the transport model linked to TripEnergy must be assigned a specific vehicle type and associated energy parameters. Accurately assigning each simulated agent with a correct vehicle type is likely too burdensome to be worthwhile for some applications, and in such cases a representative vehicle can be chosen for different vehicle categories. For cases where more detail in the vehicle fleet is required, vehicle types can be assigned to households by a discrete choice model as part of population synthesis. This functionality is especially useful for emerging integrated models where household location and vehicle ownership decisions are tied to the utilities of different transportation alternatives (*9*).

Drive Cycle Matching

We frame the process of estimating energy consumption from simulated trajectories as a prediction problem. Given limited information about a vehicle j's characteristics: $\mathscr{V}_j$, and about its trajectory: $\mathscr{U}_j$, we estimate the expected value of a vehicle's energy consumption over timestep i under those conditions: $E[E_{ij}|\mathscr{U}_j, \mathscr{V}_j]$. In this case, the information known is the vehicle's cumulative distance traveled every advance interval, and vehicle characteristics. We assume that the vehicle could have followed any speed profile over each timestep, but that the measurements at advance intervals are accurate. Given Equation 8, the goal becomes to predict the components of the moment vector $\mathbf{U}$ for each timestep given the vehicle's trajectory $\mathscr{U}$:

$$E[E_{ij}|\mathscr{U}_j, \mathscr{V}_j] = E\left[\left(\sum_{k=1}^{10} U_{ijk}V_{jk}\right)|\mathscr{U}_j, \mathscr{V}_j\right] = \sum_{k=1}^{10} E[U_{ijk}|\mathscr{U}_j]V_{jk}. \quad (10)$$

We estimate $E[\mathbf{U}_{ij}|\mathscr{U}_j]$ by searching a database of real-world drive cycles for intervals that are similar to the portion in advance interval i being estimated. The vector of moments can be calculated for each matched trajectory segment and then averaged, producing an estimate $\bar{\mathbf{U}}_{\mathbf{ij}}$ of those moments for the unknown partial trajectory, which can then be combined with the vehicle parameters $\mathbf{V}_j$ to estimate E_{ij}. This matching and averaging procedure has several advantages. It can be implemented efficiently, it does not require that detailed energy use measurements be stored for multiple vehicle types, and it is robust to modeling decisions about driving style that must be made for short-term simulations—a useful property because trajectories simulated by short-term models might not be entirely accurate for energy-consumption purposes (*3*). This solution does not directly incorporate elevation change. For networks where elevation change is expected to greatly effect energy consumption, separate moment databases can be created for different grades and accessed based on the instantaneous grade of the simulated vehicle at each timestep.

To efficiently implement this matching procedure, we create a lookup table of averaged moments that can be accessed based on binned properties of the medium-resolution trajectory. For instance, the lookup table for a simple speed-based matching scheme can be implemented by breaking each GPS drive-cycle into segments of the same duration as the advance interval, assigning each segment to a bin based on its average speed, calculating the mean moments for each bin, and then using those mean moments to calculate $E[\mathbf{U}_{ij}|\mathscr{U}_j]$. The drive cycle database used for matching consists of over 100,000 trips with 1-Hz speed measurements and has been described in detail (*2, 4-6*).

Various matching methods are possible. A one-dimensional matching scheme ($\bar{v}_t$) was tested, using only the average speed over the current advance interval. Because training data are ample, this will approximate the expected value for a vehicle's energy consumption over a timestep given only current average speed, assuming the driving behavior in the area being modeled is relatively similar to that captured in the driving behavior database and that bins are reasonably small. Two two-dimensional schemes were tested: one based on the current and previous average speeds ($\bar{v}_{t-1}, \bar{v}_t$) and one based on the average speed and average acceleration of the current advance interval ($\bar{v}_t, \bar{a}_t$), with average acceleration determined based on the instantaneous speeds at the beginning and end of the advance interval (accurate instantaneous speeds is a possible output of some but not necessarily all mesoscopic traffic simulations). Two three-dimensional matching schemes were tested: one based on the average speed over the current advance interval as well as the instantaneous speeds its the beginning and end ($\bar{v}_t, v_i, v_f$), and one based on the average speed over the preceding, current, and following advance intervals ($\bar{v}_{t-1}, \bar{v}_t, \bar{v}_{t+1}$).

As explained below, the most accurate was found to be matching based on a trajectory's average speed over a given advance interval, the previous interval, and following interval. Here, we divide speeds into 38 bins in each of the three dimensions, leading to 54,872 individual bins, each of which needs to store 8 different moments—a data structure that can be accessed quickly and uses a non-substantial amount of memory. This database is sufficiently populated if it provides a reasonably accurate expected value for the moments in each bin, a condition that requires a large set of drive cycles. Indeed, 84.5% of the bins for which there are at least 10 observations in the GPS dataset are not observed at all in the 49 drive schedules provided in the MOVES database. These behaviors not observed in the MOVES database account for 29% of the total driving time in the GPS dataset, showing the value of incorporating this additional driving behavior.

A visualization this lookup table is shown in Figure FIGURE **1**. The average speed over the advance interval being estimated is fixed for each of the three columns, the average speed for the previous time interval determines the y-position and the average speed for the next time interval determines the x-position within each subfigure. For example, the pixel at $Y = 35$, $X = 45$ in the middle (41 mph) column of Figure FIGURE 1 represents drive cycle segments averaging 41 mph and accelerating—where the previous interval averaged 35 mph and the following interval will average 45 mph. The first row of subfigures shows the number of observations in each bin, with much of the range of plausible vehicle movements having over 1,000 distinct 5-second observations. The second row shows the average value of μ_1, a moment relating to the portion of time during which the engine was active. The third row shows the average value of μ_a, a moment related to the amount of work the engine does towards acceleration.

MODEL VALIDATION

Microsimulation

The preferred matching method was chosen based on the root mean square error of fuel economy predictions, ease of applicability to mesoscopic simulations, and robustness to uncertainty in mesoscopic trajectories. Estimated energy values were compared to 'ground truth' values given by microsimulation, when the entire high-resolution trajectory is known. 20% of approximately 100,000 available 1-hz GPS trajectories were chosen as a test set. These were converted into simulated mesoscopic trajectories by downsampling them into 5-second resolution average

speeds, consistent with a mesoscopic simulation with a 5-second advance interval. An estimate for the true energy consumption was produced by simulating vehicle performance with the ADVISOR software (*7*). The vehicle simulated was a compact ICEV, with physical characteristics modeled after a 2014 Ford Focus. The vehicle model described above was then calibrated based on ADVISOR outputs—coastdown coefficients A, B, and C were estimated based on a polynomial fit to instantaneous road load, and drive cycle fuel economy measurements used for model calibration were produced by running the simulated vehicle through the EPA HWFET (Highway) and USDDS (City) drive cycles. The final vehicle model parameters used were $A: 172.8\,N$, $B: -4.676\,Ns/m$, $C: 0.5516\,Ns^2/m^2$, $m: 1406\,kg$, $P_{idle}: 11.50\,kW$, $\eta_{max}: 0.4081$. No additional auxiliary energy use is assumed.

The remaining 80% of trips were used to generate a database of binned driving behavior moments as described above, using different binning methods. The robustness of the matching methods to errors in mesoscopic trajectories is tested by adding different degrees of uncorrelated random noise to individual timesteps in the medium-resolution trajectories.

Models were compared based on root mean square estimation error for trip average fuel economy and bias in estimating the total energy consumption of the entire test set of trips, compared to ADVISOR simulations of the full high-resolution trajectory. Two other models were simulated as a comparison, neither of which is expected to be as scalable to large-scale simulations. The "Spline" model interpolated the mesoscopic trajectory to a high-resolution one using cubic splines. "Vehicle Model" assumes access to the true high-resolution trajectory but uses the simplified vehicle model described above, useful as a bound on the error introduced by the matching algorithm. Given accurate mesoscopic trajectories, the methods $(\bar{v}_t, \bar{a}_t)$, $(\bar{v}_t, v_i, v_f)$, and $(\bar{v}_{t-1}, \bar{v}_t, \bar{v}_{t+1})$ all perform roughly equivalently, with root mean square errors of trip-averaged fuel economy of approximately 0.9 mpg, compared to RMS error of 0.71 mpg given high-resolution knowledge of the trajectory and 1.08 for the spline method, and an error for the estimated total energy of all trips within 0.5% of the true value. Under increased uncertainty, the method based on three consecutive average speeds outperforms those incorporating instantaneous measurements. At high uncertainty, a spline-based method outperforms the methods based on binned moments, but all other binned methods outperform the method $(\bar{v}_t)$ based on only average speeds. A summary of these results is shown in Table 2. Given these results, the three dimensional $(\bar{v}_{t-1}, \bar{v}_t, \bar{v}_{t+1})$ method is chosen.

Aggregate Performance Measures

Additional evaluation was performed by running a simulation of a traffic network containing a variety of vehicle types, comparing fuel economy measurements for the different vehicles to EPA estimates. The transport network simulation was performed using SimMobility Midterm (*9*), a simulator linking an activity-based demand simulator with a mesoscopic, DTA supply model. TripEnergy was implemented in c++ and run concurrently with SimMobility, leading to an increase in simulation time and memory use of less than 5%. The tests were performed on the 'Virtual City' network, containing 94 nodes and 254 links, with constant elevation. The simulation was run for a full day, during which vehicles made a total of 174,594 individual trips. Four vehicle types were simulated—a 2013 Nissan Leaf (a battery-electric sedan), a 2016 Toyota Prius (a hybrid-electric sedan), a 2014 Honda Accord plug-in hybrid operating in charge depleting mode (a sedan), and a 2010 Ford F150 (a pickup truck). Additional auxiliary energy consumption of 1000 W was assumed to account for typical auxiliary use. Charging efficiency of 83.7% was assumed for the Leaf (*29*).

Vehicle fuel economies were then compared to EPA adjusted fuel economy estimates. Each trip was classified as "Highway" (more than 50% of the time spent at greater than 55 mph), or "City" for the remaining trips. Expected results were observed, with the gasoline internal combustion engine-powered F150 achieving lower fuel economy for city driving, while the hybrid-electric Prius and fully-electric Leaf typically achieving lower fuel economy for highway trips. Probability distributions for tripwise fuel economy over different trip types are shown in Figure 2.

Average fuel consumption values for each vehicle over each class of trip were compared to EPA-published "City" and "Highway" ratings, generally showing close agreement. EPA adjusted city/highway fuel economies for the Leaf, Prius, Accord PHEV in charge-sustaining mode, F150 are 126/101, 58/53, 49/45, and 15/21, respectively. In this simulation, average stop-and-go/highway fuel economies for the different vehicle types are 143/125, 59/55, 56/53, and 17/18, respectively. EPA unadjusted fuel economy ratings are used in the calibration of the efficiency parameters in the TripEnergy vehicle model, but EPA adjusted values (typically lower) are produced through a complicated process not factored into the TripEnergy model (*30*). Any agreement between TripEnergy results and EPA-adjusted values are the result of the less-energy-efficient driving and additional auxiliary use assumed in TripEnergy and present in the real world but not the unadjusted EPA tests.

DISCUSSION

This paper links an existing mesoscopic transport simulation with an energy model that can estimate the energy consumption and CO_2 emissions from personal vehicles. Given moderate resolution vehicle trajectories from a mesoscopic traffic model, TripEnergy can efficiently estimate energy consumption more accurately than simple speed and acceleration-based methods. TripEnergy offers various improvements more over widely-used methods such as MOVES: it utilizes the full detail on vehicle movements provided by mesoscopic simulations; it is computationally efficient enough to be run concurrently with a transport model; and it produces energy estimates that can be traced back to individual vehicles. In addition, because it relies primarily on independent measurements of high-resolution driving behavior, this method is less reliant than alternative models on tunable parameters governing vehicle movement, which are not typically calibrated to reproduce trajectories that are accurate from an energy perspective.

Because this model was developed to take advantage of the strengths of state-of-the-art transport simulations, we expect it to prove increasingly useful as simulations continue to evolve and be applied to new questions and research directions. These include problems where the energy consumption of vehicles needs to be integrated into agents' travel choice framework, and where energy consumption and CO_2 emissions are primary targets of study. In many of these cases, the vehicles being studied will not have detailed energy-use measurements beyond EPA-mandated tests. Specific use-cases include the development and evaluation of tools targeted at reducing individual travelers' energy use, understanding the effects of fuel economy on long-term vehicle purchasing decisions, and studying electric vehicle range and charging behavior. Additionally, the ability to calculate energy consumption from limited-resolution trajectories will be useful for contexts outside of traditional transport modeling, including suggesting energy-efficient routes given estimates of the congestion state of a traffic network, or estimating energy consumption of a trip given trajectory information captured by a smartphone.

In future work, several extensions to this analysis will be pursued. Further work is needed to quantify the degree to which mesoscopic models capture realistic traffic movement. The

impacts of user-specific driving style on energy use and the degree to which the database of driving behavior data captures this variability will also be investigated further. Finally, the vehicle model could be augmented through the inclusion of additional, higher-order moments. The additional energy estimation accuracy allowed by this modification will be assessed using onboard diagnostic recorders in on-road vehicles, and the gains in accuracy will be weighed against the complexity added to the vehicle model.

ACKNOWLEDGEMENTS
The information, data, or work presented herein was funded in part by the Advanced Research Projects Agency-Energy (ARPA-E), U.S. Department of Energy, under the TRANSNET program.

REFERENCES
[1] Casas, J., J. Perarnau, and A. Torday, The need to combine different traffic modelling levels for effectively tackling large-scale projects adding a hybrid meso/micro approach. Procedia-Social and Behavioral Sciences, Vol. 20, 2011, pp. 251–262.
[2] McNerney, J., Z. A. Needell, M. T. Chang, M. Miotti, and J. E. Trancik, TripEnergy: Estimating POV energy consumption given limited travel survey data. Transportation Research Record: Journal of the Transportation Research Board, No. 2628, 2017, pp. 58-66.
[3] da Rocha, T. V., L. Leclercq, M. Montanino, C. Parzani, V. Punzo, B. Ciuffo, and D. Villegas, Does traffic-related calibration of car-following models provide accurate estimations of vehicle emissions? Transportation Research Part D: Transport and Environment, Vol. 34, 2015, pp. 267–280.
[4] DOE National Renewable Energy Laboratory, California Household Transportation Survey. DOE-019-9889603959, 2012.
[5] Atlanta Regional Commission, Regional Travel Survey: Final Report, 2011.
[6] Texas Department of Transportation, 2002 - 2011 Regional Travel Surveys with GPS data for Abilene, Austin, El Paso, Houston Galveston, Laredo, Rio Grande Valley, San Antonio, Tyler Longview, and Wichita Falls, 2002-2011.
[7] Markel, T., A. Brooker, T. Hendricks, V. Johnson, K. Kelly, B. Kramer, M. O'Keefe, S. Sprik, and K. Wipke, ADVISOR: a systems analysis tool for advanced vehicle modeling. Journal of Power Sources, Vol. 110, No. 2, 2002, pp. 255–266.
[8] Advanced Powertrain Research Facility (APRF), Downloadable Dynamometer Database. Argonne National Laboratory (ANL), 2011.
[9] Adnan, M., F. C. Pereira, C. M. L. Azevedo, K. Basak, M. Lovric, S. Raveau, Y. Zhu, J. Ferreira, C. Zegras, and M. Ben-Akiva, SimMobility: A Multi-scale Integrated Agent-based Simulation Platform. In 95th Annual Meeting of the Transportation Research Board, 2016, 16-2691.
[10] Chiu, Y.-C., J. Bottom, M. Mahut, A. Paz, R. Balakrishna, T. Waller, and J. Hicks, Dynamic traffic assignment: A primer. Transportation Research E-Circular, No. E-C153, 2011.
[11] De Palma, A. and F. Marchal, Real cases applications of the fully dynamic METROPOLIS tool-box: an advocacy for large-scale mesoscopic transportation systems. Networks and spatial economics, Vol. 2, No. 4, 2002, pp. 347–369.
[12] Ben-Akiva, M. E., S. Gao, Z. Wei, and Y. Wen, A dynamic traffic assignment model for

highly congested urban networks. Transportation Research Part C: Emerging Technologies, Vol. 24, 2012, pp. 62 – 82.
[13] Zhou, X. and J. Taylor, DTALite: A queue-based mesoscopic traffic simulator for fast model evaluation and calibration. Cogent Engineering, Vol. 1, No. 1, 2014, p. 961345.
[14] Charypar, D., K. W. Axhausen, and K. Nagel, An event-driven queue-based microsimulation of traffic flow. ETH, Eidgenossische Technische Hochschule Zurich, IVT, Institut fur Verkehrsplanung und Transportsysteme, 2006.
[15] Bowman, J. L. and M. E. Ben-Akiva, Activity-based disaggregate travel demand model system with activity schedules. Transportation Research Part A: Policy and Practice, Vol. 35, No. 1, 2001, pp. 1–28.
[16] Samaras, C., L. Ntziachristos, and Z. Samaras, COPERT Micro: a tool to calculate the vehicle emissions in urban areas. In Transport Research Arena (TRA) 5th Conference: Transport Solutions from Research to Deployment, 2014.
[17] California Air Resource Board, 2.30 User guide: calculating emission inventories for vehicles in California, 2006.
[18] Rakha, H., K. Ahn, and A. Trani, Development of VT-Micro model for estimating hot stabilized light duty vehicle and truck emissions. Transportation Research Part D: Transport and Environment, Vol. 9, No. 1, 2004, pp. 49–74.
[19] Scora, G. and M. Barth, Comprehensive modal emissions model (CMEM), version 3.01. User guide. Centre for Environmental Research and Technology. University of California, Riverside, 2006.
[20] Saerens, B., H. Rakha, K. Ahn, and E. Van Den Bulck, Assessment of alternative polynomial fuel consumption models for use in intelligent transportation systems applications. Journal of Intelligent Transportation Systems, Vol. 17, No. 4, 2013, pp. 294–303.
[21] Assessment and Standards Division, Office of Transportation and Air Quality, Population and Activity of On-road Vehicles in MOVES2014. Draft Report EPA-420-D-15-001, U.S. Environmental Protection Agency, 2015.
[22] Frey, H. C. and B. Liu, Development and evaluation of simplified version of MOVES for coupling with traffic simulation model. In Transportation Research Board 92nd Annual Meeting, 2013, 13-1201.
[23] Zhou, X., S. Tanvir, H. Lei, J. Taylor, B. Liu, N. M. Rouphail, and H. C. Frey, Integrating a simplified emission estimation model and mesoscopic dynamic traffic simulator to efficiently evaluate emission impacts of traffic management strategies. Transportation Research Part D: Transport and Environment, Vol. 37, 2015, pp. 123–136.
[24] Zegeye, S., B. De Schutter, J. Hellendoorn, E. Breunesse, and A. Hegyi, Integrated macroscopic traffic flow, emission, and fuel consumption model for control purposes. Transportation Research Part C: Emerging Technologies, Vol. 31, 2013, pp. 158–171.
[25] Needell, Z. A., J. McNerney, M. T. Chang, and J. E. Trancik, Potential for widespread electrification of personal vehicle travel in the United States. Nature Energy, Vol. 1, 2016, p. 16112.
[26] Larminie, J. and J. Lowry, Electric Vehicle Technology Explained. John Wiley & Sons, 2004.
[27] Post, K., J. Kent, J. Tomlin, and N. Carruthers, Fuel consumption and emission modelling by power demand and a comparison with other models. Transportation Research Part A: General, Vol. 18, No. 3, 1984, pp. 191–213.

[28] United States Environmental Protection Agency, Certified Vehicle Test Results Report Data. Available http://www.epa.gov/otaq/crttst.htm, 2015.
[29] Forward, E., K. Glitman, and D. Roberts, An assessment of level 1 and level 2 electric vehicle charging efficiency. Vermont Energy Investment Corporation Transportation Efficiency Group, 2013.
[30] Fuel Economy Labeling of Motor Vehicle Revisions to Improve Calculation of Fuel Economy Estimates. Office of Transportation and Air Quality, US EPA, 2006.
[31] Ahn, K. and H. Rakha, The effects of route choice decisions on vehicle energy consumption and emissions. Transportation Research Part D: Transport and Environment, Vol. 13, No. 3, 2008, pp. 151 – 167.

Model	Resolution Needed	Energy Method
COPERT-micro (*16*)	Link	Speed
EMFAC (*17*)	Trip	Speed
ADVISOR(*7*)	High-resolution	Microsimulation
VT-Micro (*31*)	High-resolution	Speed/Acceleration
MOVES County (*21*)	Link	Vehicle Specific Power
MOVES Project (*21*)	High-resolution	Vehicle Specific Power
MOVESlite (*23*)	High-resolution	Vehicle Specific Power
VT-Macro (24)	Link	Speed/Acceleration
Zhou et al (*23*)	Mesoscopic	Vehicle Specific Power

TABLE 1 Summary of Selected Methods to Calculate Energy Based on Transport Network Simulations

Estimation Method	No noise		±1 mph noise		±2 mph noise	
	RMS (mpg)	Total Energy	RMS (mpg)	Total Energy	RMS (mpg)	Total Energy
Spline	1.08	-2.20%	0.96	-1.20%	1.13	1.98%
$(\bar{v}_t)$	2.47	-0.78%	2.47	-0.73%	2.46	-0.55%
$(\bar{v}_{t-1}, \bar{v}_t)$	1.33	-0.65%	1.44	-0.19%	1.92	2.19%
$(\bar{v}_t, \bar{a}_t)$	0.93	-0.36%	1.08	0.50%	1.64	3.40%
$(\bar{v}_t, v_i, v_f)$	0.88	-0.40%	1.33	1.01%	2.39	4.12%
$(\bar{v}_{t-1}, \bar{v}_t, \bar{v}_{t+1})$	0.9	-0.45%	0.99	-0.06%	1.47	2.24%
Vehicle Model	0.71	-0.28%	na	na	na	na

TABLE 2 Performance of Different Matching Methods, Evaluated Against ADVISOR
(na = not applicable, as "Vehicle Model" assumes perfect knowledge of the vehicle trajectory)

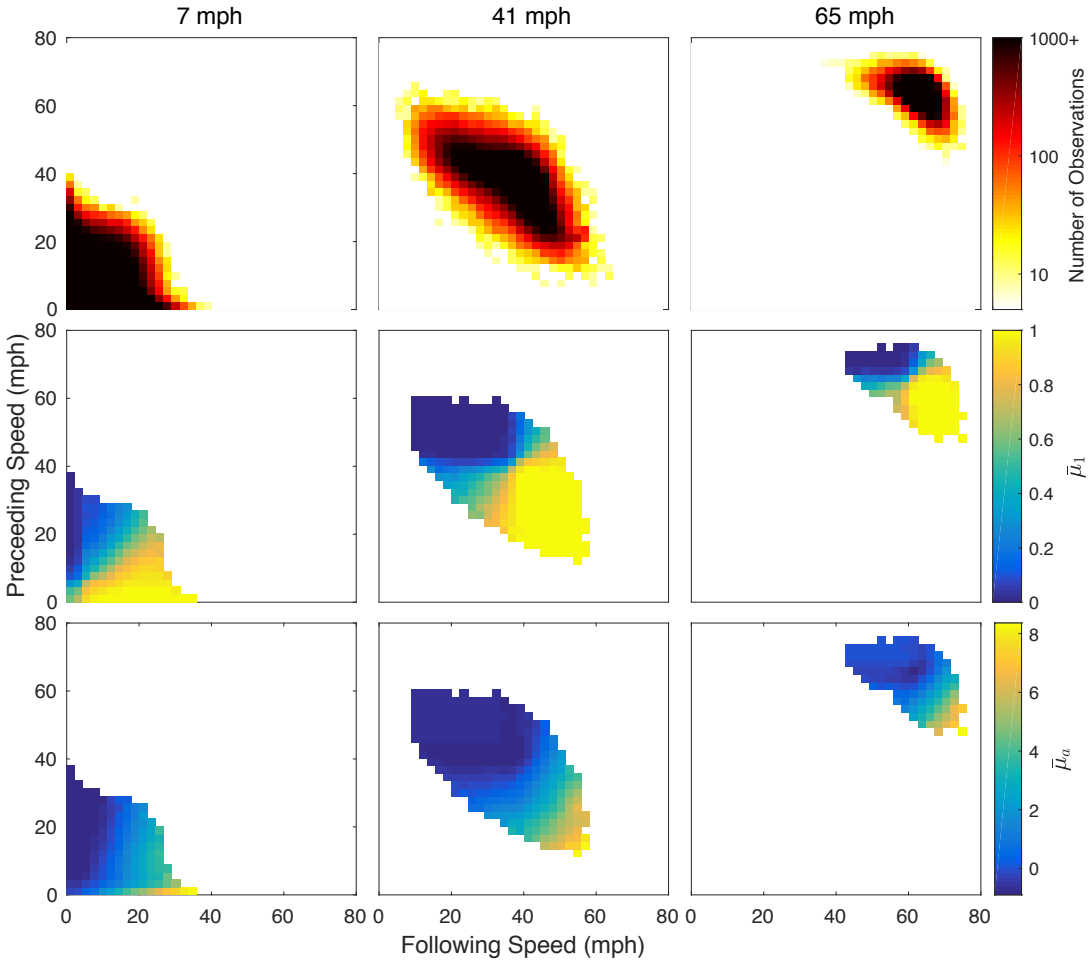

FIGURE 1 Visualization of the lookup table of drive cycle moments produced by matching on three consecutive average speeds, for a 5-second advance interval.

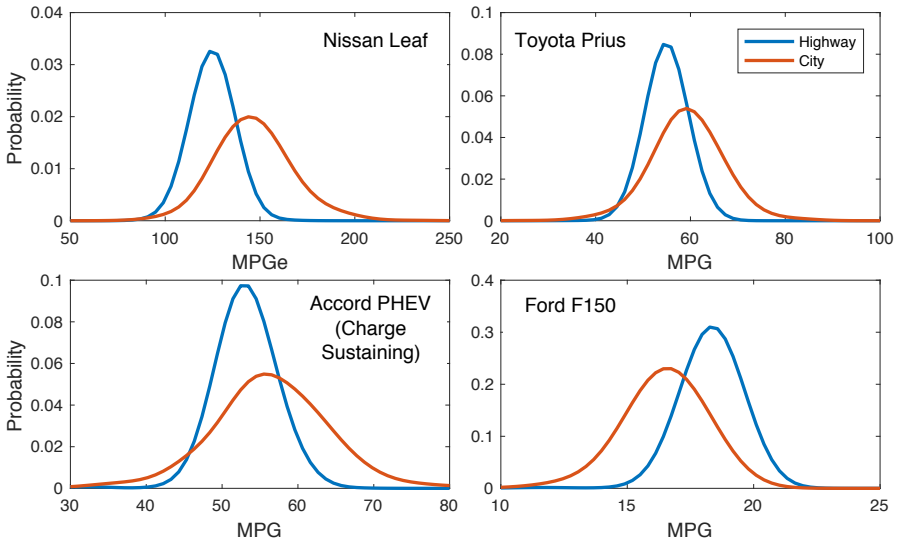

FIGURE 2 Distribution of trip-averaged fuel economies for different vehicle types, simulated with SimMobility over the "Virtual City" road network, measured in miles per gallon (MPG) for gasoline powered vehicles and miles per gallon equivalent (MPGe) for electric vehicles.